Acta Crystallographica Section D
Biological Crystallography
ISSN 0907-4449

Structure of the *Bacillus subtilis* OhrB hydroperoxide-resistance protein in a fully oxidized state

David R. Cooper, Yogesh Surendranath, Yancho Devedjiev, Jakub Bielnicki and Zygmunt S. Derewenda*

Department of Molecular Physiology and Biological Physics, University of Virginia and the PSI2 Integrated Center for Structure–Function Innovation Charlottesville, Virginia 22908, USA

Correspondence e-mail: zsd4n@virginia.edu

Received 12 September 2007
Accepted 15 October 2007

PDB Reference: organic hydroperoxide-resistance protein B, 2bjo, r2bjosf.

The crystal structure of the fully oxidized form of the *Bacillus subtilis* organic hydroperoxide-resistance (OhrB) protein is reported at 2.1 Å resolution. The electron density reveals an intact catalytic disulfide bond (Cys55–Cys119) in each of the two molecules, which are intertwined into a canonical obligate dimer. However, the stereochemistry of the disulfides is unorthodox and strained, suggesting that they are sensitive to reducing agents. A deep solvent-accessible gorge reaching Cys55 may represent the access route for the reductant.

1. Introduction

Following infection, plants and animals respond with an oxidative burst intended to damage the DNA, lipids and proteins of the infecting microorganism (Talarczyk & Hennig, 2001; Wojtaszek, 1997). To countervail this threat, bacteria have evolved complex mechanisms to detoxify reactive oxygen species such as H_2O_2, superoxide anion radicals, the hydroxide radical and organic hydroperoxides (OHPs) (Storz *et al.*, 1990).

OHPs constitute one of the most bacteriotoxic classes of compounds that result from lipid peroxidation, leading to altered membrane properties (Akaike *et al.*, 1992). The main bacterial defense mechanism against OHPs involves alkyl hydroperoxide reductase, a member of the peroxiredoxin family (Poole, 2005), but the second line of defense is the hydroperoxide-resistance protein Ohr. This protein was originally discovered in *Xanthomonas campestris*, where deletion mutants were found to be highly sensitive to OHPs (Mongkolsuk *et al.*, 1998). It has since been found in a number of pathogenic bacterial species (Atichartpongkul *et al.*, 2001).

The Ohr proteins are thiol-dependent peroxidases containing two conserved cysteines which catalyze the reduction of alkyl peroxides to alcohols with the concomitant release of water and oxidation of the cysteines to a disulfide. *In vitro*, the reaction requires dithiols such as DTT. Several crystal structures of these enzymes have been studied in recent years, including those from *Pseudomonas aeruginosa* (Lesniak *et al.*, 2002), *Deinococcus radiodurans* (Meunier-Jamin *et al.*, 2004) and *Xylella fastidiosa* (Oliveira *et al.*, 2006). The Ohr protein is an obligate homodimer consisting of two intertwined polypeptide chains, each made up of ∼140 amino acids. Two six-stranded β-sheets, each made up of three strands from one chain and three from the other, fold around the core of the homodimer, which is made up of two α-helices, each contributed by one of the polypeptide chains. One of the active-site cysteines is located midway through the sequence, in the central part of the core helix, whereas the second is located towards the C-terminus in an abrupt kink between two shorter helices. There are typically ∼65 intervening amino acids between the two cysteines.

The broadly defined Ohr family also includes the OsmC proteins, which share about 20% amino-acid identity with the Ohr-family members; they were originally thought to constitute part of a response to osmotic shock, but were subsequently identified as peroxidases with a catalytic mechanism similar to that of Ohr (Atichartpongkul *et al.*, 2001; Gutierrez & Devedjian, 1991). Several crystal structures of OsmC-family members have also been determined (Lesniak *et al.*, 2003; Meunier-Jamin *et al.*, 2004; Rehse *et al.*, 2004; Shin *et al.*, 2004).

This wealth of structural information made it possible to propose a general catalytic mechanism for Ohr proteins. According to this mechanism, in its resting reduced form the enzyme is stabilized by a salt bridge between a thiolate of the first (*i.e.* catalytic) cysteine and an arginine located in the $\beta1$–$\beta2$ turn. This conformation is in turn held in position by a neighboring glutamate. The catalytic cysteine is oxidized to sulfenic acid upon reduction of the substrate organic peroxide, which is bound in a hydrophobic cleft. This form is transient and an immediate attack follows by the sulfhydryl of the second cysteine, with the resulting formation of a disulfide. During this reaction, the loop containing the arginine moves away from the active site. The final step involves the reduction of the enzyme, although neither the nature of the reducing agent nor the identity of the enzymes involved in this pathway are known.

The available crystal structures of Ohr proteins exemplify snapshots along the catalytic pathway. They include a fully reduced state (Lesniak *et al.*, 2002), a mixture of reduced and oxidized states (Meunier-Jamin *et al.*, 2004) and one in which the cysteines were oxidized to sulfonic acid (Oliveira *et al.*, 2006). The fully oxidized state, a transient intermediate remaining after the release of the reaction product, has not been described.

In *Bacillus subtilis*, an Ohr homologue seems to play a primary role in defense against OHPs (Fuangthong *et al.*, 2001). *B. subtilis* is one of the few bacteria that have two homologues of Ohr as well as an OsmC (Atichartpongkul *et al.*, 2001). The OhrB protein was selected as a target for the high-throughput pipeline by the Midwest Center for Structural Genomics, but failed to crystallize in routine screens. It was subsequently selected for crystallization by the surface entropy-reduction (SER) protocol (Derewenda & Vekilov, 2006; Goldschmidt *et al.*, 2007). A triple mutant, K34A,K35A,E36A, crystallized easily and the structure was solved by molecular replacement and refined at 2.1 Å. Somewhat unexpectedly, the refined model revealed a fully oxidized state of the enzyme with intact disulfide bonds. Here, we discuss the implications of this structure for the catalytic mechanism of the Ohr family.

2. Materials and methods

2.1. Protein expression and purification

The pMCSG7 expression vector containing the *B. subtilis* OhrB gene with an N-terminal His_6 tag (Apc1270) was obtained from the Midwest Center for Structural Genomics. Expression was carried out in *Escherichia coli* BL21(DE3) strain in Luria–Bertani medium (LB). Wild-type and mutant proteins were produced after induction with 1 m*M* IPTG at 293 K when the OD_{600} reached 5.0. Cells were harvested by centrifugation and lysed by sonication. The protein was initially purified using nickel-affinity chromatography (Ni–NTA agarose column; Qiagen) and subjected to rTEV proteolysis at 283 K for 24 h to cleave the His tag. Samples were again run through an Ni-affinity column to isolate pure untagged protein, which was dialyzed for 12 h against a buffer consisting of 20 m*M* Tris–HCl pH 8.0. Pure native protein was concentrated to 10–12 mg ml^{-1}. β-Mercaptoethanol was added to a final concentration of 2.5 m*M* and protein samples were stored at 193 K. The QuikChange protocol (Stratagene Inc.) was used to create a K34A,K35A,E36A mutant. This SER variant was purified as described above.

2.2. Crystallization and data collection

The wild type and SER variant were screened using a custom-made sparse-matrix screen derived from published data-mining experiments (Kimber *et al.*, 2003; Page & Stevens, 2004; Page *et al.*, 2003; Cooper *et al.*, 2007). No crystals were observed for the wild-type protein, while the mutated protein yielded diffraction-quality crystals straight from the screen. The optimal conditions were 1.0 *M* sodium citrate and 0.1 *M* sodium cacodylate pH 6.5. Data were collected using an in-house system consisting of an Enraf–Nonius FR591 rotating-anode generator with Cu target equipped with Osmic confocal mirrors and a Rigaku R-AXIS IV imaging plate. The Matthews coefficient (Matthews, 1968) was 2.2 Å^3 Da^{-1}, consistent with the presence of two polypeptide chains per asymmetric unit and 42.6% solvent content. Processing and merging of the data were carried out with *HKL*-2000 (Otwinowski & Minor, 1997). Further details are given in Table 1.

Table 1
OhrB data-collection statistics.

Values in parentheses are for the highest resolution shell.

Space group	*P*1
Unit-cell parameters (Å, °)	a = 35.34, b = 41.43, c = 44.60, α = 84.5, β = 91.5, γ = 73.9
Resolution (Å)	30.0–2.10 (2.18–2.10)
Total reflections	28333
Unique reflections	12453 (656)
Redundancy	2.3 (2.0)
Completeness (%)	88.6 (46.6)
R_{sym}† (%)	3.9 (25.6)
Average $I/\sigma(I)$	22.8 (3.0)
Refinement statistics	
Resolution (Å)	30.00–2.10 (2.15–2.10)
Reflections (working)	11511
Reflections (test)	942
R_{work}‡ (%)	16.1 (24.2)
R_{free}‡ (%)	19.9 (31.0)
No. of waters	218
R.m.s. deviation from ideal geometry	
Bonds (Å)	0.010
Angles (°)	2.430
Average temperature factor (Å^2)	
Main chain	25.9
Side chains	29.5
Waters	35.2

† $R_{sym} = \sum_{hkl} |I - \langle I\rangle| / \sum_{hkl} I$. ‡ R_{work} or $R_{free} = \sum_{hkl} \big||F_{obs}(hkl)| - |F_{calc}(hkl)|\big| / \sum_{hkl} |F_{obs}(hkl)|$.

2.3. Structure solution and refinement

The 2.0 Å model of the *P. aeruginosa* Ohr protein (PDB code 1n2f; Lesniak *et al.*, 2002) provided the basis of a molecular-replacement model. After initial trials with the intact dimer from 1n2f, the program *SEAMAN* (Kleywegt, 1996) was used to truncate non-identical residues to serine, alanine or glycine. The structure was solved by molecular replacement with this model using *AMoRe* (Navaza, 1994). Following several cycles of refinement, electron-density maps revealed a partial structure with density missing for residues 68–76 and 107–113 in both chains. Subsequent iterative cycles of model building with *RESOLVE* and refinement with *REFMAC*5 were performed using the script provided with *RESOLVE* and the incomplete model as a starting point (Terwilliger, 2003). This process improved the maps dramatically, and although no single resulting structure contained all of the missing residues, the missing fragments were present in some of *RESOLVE*'s intermediate structures. A combination of 'cut-and-paste' model building and manual refinement resulted in a complete structure. This iterative process allowed the refinement, which had previously stalled with an R_{free} of around 42%, to converge with crystallographic R and R_{free} values of 15.8% and 19.9%, respectively. The program *O* (Jones *et al.*, 1991) was used for map interpretation and manual model building. Final models were also refined with *REFMAC*5 (Murshudov *et al.*,

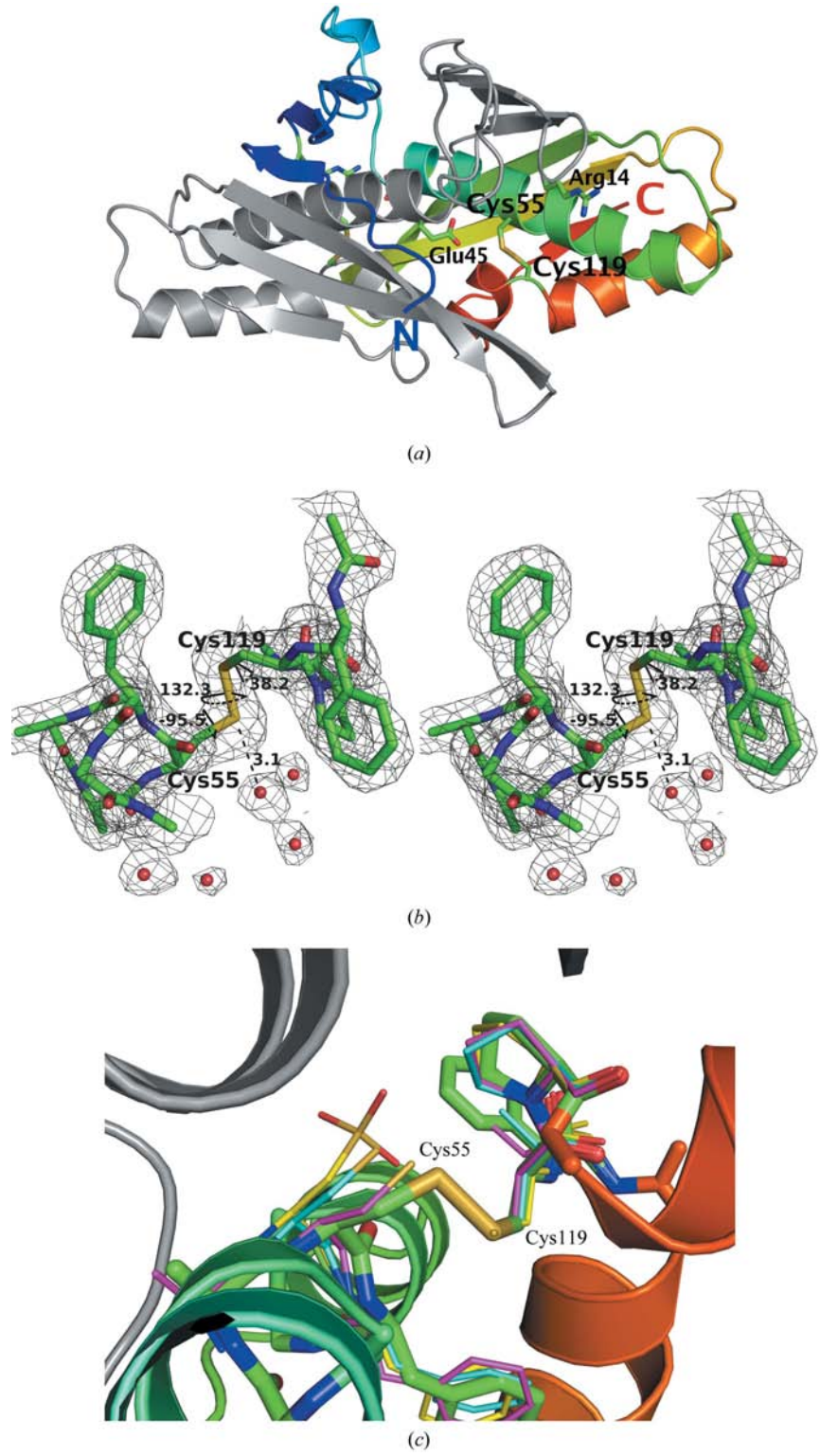

Figure 1
The structure of OhrB. (*a*) OhrB is shown in a ribbon representation with monomer *A* colored from blue to red. The locations of key active-site residues are shown. (*b*) A wall-eyed stereoview of the active-site disulfide of chain *A* with a σ_A-weighted $2mF_{obs} - DF_{calc}$ electron-density map contoured at 1σ. Torsion angles and distances described in the text are shown. (*c*) Superposition of other Ohr structures. The perspective of this figure is from the inside of the OhrB dimer looking out through the gorge. The *B. subtilis* OhrB is colored as above, with green C atoms. The active sites of other Ohr structures are shown for comparison. The *P. aeruginosa* protein (PDB code 1nf2; Lesniak *et al.*, 2002) is shown with cyan C atoms, that from *D. radiodurans* (PDB code 1usp; Meunier-Jamin *et al.*, 2004) has magenta C atoms and that from *X. fastidiosa* (PDB code 1zb8; Oliveira *et al.*, 2006), in which the cysteines have been oxidized to sulfonic acids, has yellow C atoms.

1997). Individual isotropic displacement parameters (*B* factors) were used throughout. The validation of the model was carried out using *MOLPROBITY* (Lovell *et al.*, 2003) and *PROCHECK* (Laskowski *et al.*, 1993). Further details are given in Table 1. Figures were prepared with *PyMOL* (http://www.pymol.org).

3. Results and discussion

3.1. Engineering a crystallizable OhrB mutant

A tripeptide with high conformational entropy, K34,K35,E36, was selected as a target for the entropy-reduction protocol and the three residues were mutated to alanines. We have recently reported a web server, SERp (http://nihserver.mbi.ucla.edu/SER/), that allows the automated analysis of a protein sequence and the identification of suitable mutation sites for the preparation of crystallizable protein variants (Goldschmidt *et al.*, 2007). Although we initially picked the high-entropy site manually, we subsequently checked this choice against the server's prediction. Based on the side-chain entropy profile and secondary-structure prediction, the server identifies only three sites suitable for mutagenesis in OhrB: the above triple site (with the highest score of 11.5), K64,E65 (score 9.3) and E106,K107,Q109 (score 6.63). All other minor sites have scores below 4.0. Thus, our original choice was consistent with the server's prediction.

3.2. Overview of the structure and functional implications

The *B. subtilis* OhrB structure closely resembles the previously reported structures, as might be expected from the amino-acid sequence similarities (Fig. 1*a*). The crystal structure is of high quality, with a conventional crystallographic *R* factor of 15.8% and an R_{free} of 19.9% (Table 1). The *P*1 unit cell is occupied by a homodimer, with interpretable electron density observed for all residues from Ala2 to Lys136 in both chains and 228 water molecules.

The electron density for the functionally important disulfide bond Cys55–Cys119 is clearly resolved in both molecules and is consistent with a fully oxidized state. The refined model shows that the S—S bond lengths are ∼2.1 Å, which is also consistent with complete oxidation (Fig. 1*b*). This clearly differentiates our structure from those reported previously for several Ohr homologues (Fig. 1*c*), as well as from the previously determined structures of OsmC-family members (Lesniak *et al.*, 2003; Meunier-Jamin *et al.*, 2004; Rehse *et al.*, 2004; Shin *et al.*, 2004). This is most likely to be the consequence of two independent factors. Firstly, we did not use dithiothreitol (DTT) or other reducing agents in the crystallization screens. Secondly, we collected

good-quality X-ray data using an in-house generator, with accordingly lower flux and a much smaller radiation-damage effect. It has been noted previously that the mixed oxidation state observed in the *D. radiodurans* Ohr structure may have been a specific consequence of radiation damage (Meunier-Jamin *et al.*, 2004).

The oxidized state is believed to be a transient intermediate remaining after the release of the reaction products (Oliveira *et al.*, 2006; Lesniak *et al.*, 2002). The protein reverts to the reduced form as a result of poorly understood reduction pathways. In this context, the stereochemistry of the disulfide bonds in the *B. subtilis* crystal structure is noteworthy. A recent analysis of 837 native disulfide bonds (Pellequer & Chen, 2006) shows that the S—S bond stereochemistry is highly conserved in naturally occurring disulfide bridges. The average $C^{\alpha}-C^{\alpha}$ distance is 5.4 ± 0.7 Å, the $C^{\beta}-C^{\beta}$ distance is 3.8 ± 0.2 Å and the S—S bond distance is 2.04 ± 0.07 Å. The dihedral angles are also highly restricted, with the $C^{\beta}-S^{\gamma}-S^{\gamma}-C^{\beta}$ (χ_S) angle close to ±90 ± 17° and the $C^{\alpha}-C^{\beta}-S^{\gamma}-S^{\gamma}$ angles (χ_1 and χ_2) both clustering distinctly around −60° (Dani *et al.*, 2003). In contrast to this paradigm, the *B. subtilis* Ohr bonds are both 'asymmetric', so that the Cys55 χ_1 angle is within the expected range (−94 and −95°) whilst the two Cys119 χ_2 angles assume rare and unfavorable values (38 and 46° in chains *A* and *B*, respectively). The χ_S angles also deviate from the canonical range and assume values of 132 and 133° in the *A* and *B* chains, respectively. This stereochemistry results in an unusually long $C^{\beta}-C^{\beta}$ distance of 4.7 Å, which is outside the range of values found in naturally occurring S—S bridges. We suspect that this has functional consequences in that the unfavorable stereochemistry renders this disulfide less stable and susceptible to reducing agents.

In this context, we analyzed the solvent-accessible surfaces. There is a deep gorge extending from the surface of the dimer into the interface between the two central helices. The gorge extends all the way into the immediate proximity of the disulfide and consequently the S^{γ} of Cys55 (but not that of Cys119) is solvent-accessible on the distal side of the disulfide. Furthermore, the bottom of the gorge adjacent to Cys55 is occupied by several ordered water molecules with an overall stereochemistry that is remarkably well preserved in both chains. One of these water molecules is in direct proximity to Cys55 S^{γ}, with an $O-S^{\gamma}$ distance of 3.1 Å in the *A* molecule (Fig. 1*b*). In the *B* molecule the density is continuous at a lower level between S^{γ} and the water O atom, so that the latter refines even closer at 2.5 Å, although this is probably a refinement artifact at 2.1 Å resolution. The temperature (*B*) factors and local environment (including two water molecules bound *via* hydrogen bonds at 2.9 and 3.2 Å) are all consistent with the electron density representing a genuine water molecule. It is not clear to us what functional implication may stem from the presence of these waters close to the disulfide.

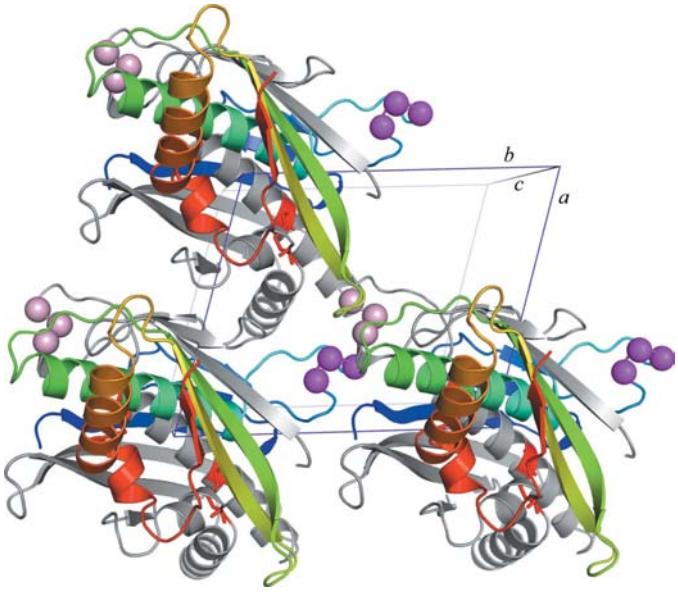

Figure 2
Crystal packing. In each dimer, monomer *A* is colored from blue to red and monomer *B* is gray. The magenta and pink spheres show the locations of the Ala substitutions of this SER variant.

In addition to the conserved cysteines, the active site of Ohr proteins contains two other residues that are believed to play a role in the stabilization of the reduced ground state. In the *B. subtilis* protein, these are Arg14 and Glu45. It has been shown that in the reduced form of the *P. aeruginosa* protein, Arg18 (equivalent to Arg14 in *B. subtilis*) is hydrogen bonded to Cys60 (Cys55 in *B. subtilis*) and is engaged in an intimate salt bridge with Glu50 (Lesniak *et al.*, 2002). Such hydrogen bonds, involving either Arg, Tyr or main-chain amides, are known to stabilize the thiolate and lower the pK_a of the Cys residue (Liu *et al.*, 1992). It seems likely that the role of the conserved Glu is to position the side chain of the arginine in a manner favorable for donating a hydrogen bond to the catalytically essential Cys. Upon formation of the transient disulfide, the assisting arginine is expelled from the active site and the loop which carries it undergoes a conformational change (Oliveira *et al.*, 2006). Interestingly, in the *B. subtilis* structure the two monomers of OhrB, while showing identical Cys55–Cys119 disulfides, reveal two distinct conformations for the Arg-carrying loop, attesting to the intrinsic flexibility of this part of the structure. The *B* factors for these Arg side chains are almost double the average *B* factor for this structure.

In conclusion, the *B. subtilis* Ohr crystal structure is largely consistent with the mechanism inferred from the previously published investigations, but extends our knowledge of the system to include detailed stereochemistry of the disulfide bonds in the transient intermediate and provides a molecular explanation of their sensitivity to reducing agents.

3.3. Crystal contacts and molecular packing

The loop containing the mutations K34A,K35A,E36A (which we refer to as the Ala loop) adopts slightly different conformations in the two molecules of the homodimer and packs in the crystal lattice with two different sets of crystal contacts. As seen in many other SER structures, the mutated residues of this SER variant participate in the crystal contacts (Fig. 2). In this case, the contacts mediated by the Ala loop are heterotypic in nature, *i.e.* the mutated site interacts with a different epitope on its neighbors. The Ala loop of monomer *B* (pink spheres in Fig. 2) is wedged in a crevice formed by three elements: the monomer *A* Ala loop of the symmetry mate generated by translation along *b* and two protrusions from a second dimer along the *ab* diagonal. One of these protrusions is the hairpin loop (residues Asp84–Gly89) at the end of the second β-sheet of chain *A* and the other is the C-terminal end of the Cys55-containing core helix of chain *B*. The two contacts are sufficient to pack molecules in the *ab* plane, but an additional contact is required to bring the molecules together along *c*. This contact is rich in large hydrophilic amino acids, including Arg105, Lys136, Glu134, Lys101 and others. In conclusion, the structure supports the notion that mutations of high conformational entropy side chains to alanines generate more easily crystallizable protein variants.

We thank Dr Andrzej Joachimiak and Dr Frank Collart (Argonne National Laboratory) for providing the expression plasmid for the

B. subtilis OhrB. This work was supported by NIH Grant GM62615 to ZSD and by the Integrated Center for Structure–Function Innovation funded by the PSI2 Initiative (NIH U54 GM074946).

References

Akaike, T., Sato, K., Ijiri, S., Miyamoto, Y., Kohno, M., Ando, M. & Maeda, H. (1992). *Arch. Biochem. Biophys.* **294**, 55–63.
Atichartpongkul, S., Loprasert, S., Vattanaviboon, P., Whangsuk, W., Helmann, J. D. & Mongkolsuk, S. (2001). *Microbiology*, **147**, 1775–1782.
Cooper, D. R., Boczek, T., Grelewska, K., Pinkowska, M., Sikorska, M., Zawadzki, M. & Derewenda, Z. (2007). *Acta Cryst.* D**63**, 636–645.
Dani, V. S., Ramakrishnan, C. & Varadarajan, R. (2003). *Protein Eng.* **16**, 187–193.
Derewenda, Z. S. & Vekilov, P. G. (2006). *Acta Cryst.* D**62**, 116–124.
Fuangthong, M., Atichartpongkul, S., Mongkolsuk, S. & Helmann, J. D. (2001). *J. Bacteriol.* **183**, 4134–4141.
Goldschmidt, L., Cooper, D. R., Derewenda, Z. S. & Eisenberg, D. (2007). *Protein Sci.* **16**, 1569–1576.
Gutierrez, C. & Devedjian, J. C. (1991). *J. Mol. Biol.* **220**, 959–973.
Jones, T. A., Zou, J.-Y., Cowan, S. W. & Kjeldgaard, M. (1991). *Acta Cryst.* A**47**, 110–119.
Kimber, M. S., Vallee, F., Houston, S., Necakov, A., Skarina, T., Evdokimova, E., Beasley, S., Christendat, D., Savchenko, A., Arrowsmith, C. H., Vedadi, M., Gerstein, M. & Edwards, A. M. (2003). *Proteins*, **51**, 562–568.
Kleywegt, G. J. (1996). *Jnt CCP4/ESF–EACBM Newsl. Protein Crystallogr.* **32**, 32–36.
Laskowski, R. A., MacArthur, M. W., Moss, D. S. & Thornton, J. M. (1993). *J. Appl. Cryst.* **26**, 283–291.
Lesniak, J., Barton, W. A. & Nikolov, D. B. (2002). *EMBO J.* **21**, 6649–6659.
Lesniak, J., Barton, W. A. & Nikolov, D. B. (2003). *Protein Sci.* **12**, 2838–2843.
Liu, S., Zhang, P., Ji, X., Johnson, W. W., Gilliland, G. L. & Armstrong, R. N. (1992). *J. Biol. Chem.* **267**, 4296–4299.
Lovell, S. C., Davis, I. W., Arendall, W. B. III, de Bakker, P. I., Word, J. M., Prisant, M. G., Richardson, J. S. & Richardson, D. C. (2003). *Proteins*, **50**, 437–450.
Matthews, B. W. (1968). *J. Mol. Biol.* **33**, 491–497.
Meunier-Jamin, C., Kapp, U., Leonard, G. A. & McSweeney, S. (2004). *J. Biol. Chem.* **279**, 25830–25837.
Mongkolsuk, S., Praituan, W., Loprasert, S., Fuangthong, M. & Chamnongpol, S. (1998). *J. Bacteriol.* **180**, 2636–2643.
Murshudov, G. N., Vagin, A. A. & Dodson, E. J. (1997). *Acta Cryst.* D**53**, 240–255.
Navaza, J. (1994). *Acta Cryst.* A**50**, 157–163.
Oliveira, M. A., Guimaraes, B. G., Cussiol, J. R., Medrano, F. J., Gozzo, F. C. & Netto, L. E. (2006). *J. Mol. Biol.* **359**, 433–445.
Otwinowski, Z. & Minor, W. (1997). *Methods Enzymol.* **276**, 307–326.
Page, R., Grzechnik, S. K., Canaves, J. M., Spraggon, G., Kreusch, A., Kuhn, P., Stevens, R. C. & Lesley, S. A. (2003). *Acta Cryst.* D**59**, 1028–1037.
Page, R. & Stevens, R. C. (2004). *Methods*, **34**, 373–389.
Pellequer, J. L. & Chen, S. W. (2006). *Proteins*, **65**, 192–202.
Poole, L. B. (2005). *Arch. Biochem. Biophys.* **433**, 240–254.
Rehse, P. H., Ohshima, N., Nodake, Y. & Tahirov, T. H. (2004). *J. Mol. Biol.* **338**, 959–968.
Shin, D. H., Choi, I.-G., Busso, D., Jancarik, J., Yokota, H., Kim, R. & Kim, S.-H. (2004). *Acta Cryst.* D**60**, 903–911.
Storz, G., Tartaglia, L. A., Farr, S. B. & Ames, B. N. (1990). *Trends Genet.* **6**, 363–368.
Talarczyk, A. & Hennig, J. (2001). *Cell. Mol. Biol. Lett.* **6**, 955–970.
Terwilliger, T. C. (2003). *Acta Cryst.* D**59**, 1174–1182.
Wojtaszek, P. (1997). *Biochem. J.* **322**, 681–692.